

# Simulation of Gel-Type Multicomponent Fixed-Bed Ion Exchange

György Kossa<sup>1</sup>, József Dobor<sup>2</sup>, György Pátzay<sup>3\*</sup>

<sup>1</sup> Board of Trustees of the Gróf Tisza István Foundation for the University of Debrecen, Egyetem tér 1, H-4032 Debrecen, Hungary

<sup>2</sup> Department of Industrial Safety, Institute of Disaster Management, Faculty of Law Enforcement, Ludovika University of Public Service, Hungária krt. 9-11, H-1101 Budapest, Hungary

<sup>3</sup> Department of Chemical and Environmental Process Engineering, Faculty of Chemical Technology and Biotechnology, Budapest University of Technology and Economics, Műegyetem rkp. 3, H-1111 Budapest, Hungary

\* Corresponding author, e-mail: [patzay.gyorgy@vbk.bme.hu](mailto:patzay.gyorgy@vbk.bme.hu)

Received: 23 November 2025, Accepted: 04 March 2026, Published online: 27 April 2026

## Abstract

The modelling of fixed-bed, multicomponent ion exchange processes using gel-type resins was investigated. Based on the earlier developed kinetic model a complex, fixed-bed ion exchange model, utilizing the Nernst-Planck diffusion kinetics, was developed. A computer program was created to describe multicomponent breakthrough and elution curves for gel-type ion exchangers using the Nernst-Planck diffusion equation. By calculating breakthrough curves for two-, three- and five-component ion exchange systems, the accuracy of the model was successfully tested. By comparison, our simulation results, which were based on the experimentally measured breakthrough data, showed suitable fits.

## Keywords

multicomponent, ion exchange, breakthrough, Nernst-Planck diffusion, simulation

## 1 Introduction

Computational and theoretical modelling has become an important tool for the characterization, development, and validation of ion exchange packed beds. Relevant breakthrough curves would provide much valuable information on designing a fixed-bed ion exchange process in field applications. Characteristic performances of fixed-bed ion exchange depend on various parameters, e.g., composition, concentration, and flow rate of feed solution, type, total capacity, and initial ionic form of ion exchanger, fixed-bed height, and operation temperature. Various research papers aimed to model the multicomponent mixtures separation by fixed-bed ion exchange [1–6]. An examination of the literature reveals that references to multicomponent ion exchange in fixed-bed columns are rare. One of the reasons for the lack of experimental multicomponent breakthrough curves has been difficulties in analytical measurements. The Nernst-Planck model for intraparticle mass transfer in ion exchange takes into account the contributions of diffusion and electrical potential, while Fick's law considers only diffusion, so the Nernst-Planck model is more realistic for multicomponent ion exchange kinetics.

At the Department of Chemical and Environmental Process Engineering (earlier Department of Chemical Technology) of Budapest University of Technology and Economics, we have developed several programs and models for industrial use. As discussed earlier, we constructed models and computer programs for the simulation of scaling in multicomponent geothermal water (program GEOPROF) [7], a model for the simulation of leaching processes from solid radioactive waste samples (ILT15, ILT20) [8, 9], models for the simulation of multicomponent sorption processes in porous packed columns [10, 11], and stirred bath [12]. We have also developed a simulation program to describe multicomponent ion exchange kinetics according to the Nernst-Planck model in gel-type ion exchange beads [13]. The goal of this research work is to develop, describe and investigate the accuracy and reliability of multicomponent ion exchange models for gel-type ion exchangers in fixed-bed, describe mass transfer processes and find effective solution methods for coupled partial differential equations by finite difference techniques. Using our earlier developed Nernst-Planck kinetic

model for gel-type ion exchange particles [13], in collaboration with partner universities, we created a fixed-bed ion exchange model that utilized the Nernst-Planck diffusion coefficients. A computer code was constructed. We now present the simulation results of the models developed.

## 2 Construction of a new model

### 2.1 The new model

In ion exchange separation processes particular attention is given to simulating behavior. A reliable simulation model is of great help in verifying the diffusional behavior of different ion exchangers, which is a considerable reduction in experimental work. In our developed model we used a gel-type multicomponent ion exchange model. We constructed a model for simulating multicomponent ion exchange in a fixed bed by describing multicomponent concentration profiles within the spherical ion exchange beads, along the fixed-bed column, and the multicomponent breakthrough curves. The developed model utilizes constant or variable diffusion coefficients according to the Nernst-Planck model for the solid phase and can calculate a complete ion exchange cycle series, including feeding until breakthrough, backwash with water with co- or counter-current flow and elution with a co- or counter-current eluent flow. The results are multicomponent saturation breakthrough-, co-current- and counter-current elution curves for gel-type ion exchangers in a fixed bed, as well as the concentration profiles in each cycle, steps in the particles and along the column. Considering the saturation stroke in the cyclic sorption process a set of continuity, rate and equilibrium equations can be written for each component of ion exchange or adsorption. In isothermal operations no longitudinal or radial diffusion effect was assumed for the continuity equation. For the rate equations it was assumed that the solid and liquid-film diffusion may be the rate-determining step. The continuity and rate equations for ionic component  $i$ , in an ion exchange column filled with spherical ion exchange beads, neglecting axial dispersion, are as shown in Eqs. (1) and (2):

$$\frac{\partial C_i}{\partial t} + \frac{3 \cdot K_{fi}}{\varepsilon R_p} \cdot (C_i - C_i^*) + \frac{U}{\varepsilon} \cdot \frac{\partial C_i}{\partial l} = 0 \quad (1)$$

$$\frac{\partial q_i}{\partial t} = D_{si} \cdot \frac{\partial^2 q_i}{\partial r^2} + 2 \cdot \frac{D_{si}}{r} \cdot \frac{\partial q_i}{\partial r} \quad (2)$$

where  $C_i$  is the liquid phase concentration of component  $i$  in the fixed bed (milliequivalents/cm<sup>3</sup>, abbreviated as meq/cm<sup>3</sup>),  $C_i^*$  is the equilibrium liquid

phase concentration at the particle surface (meq/cm<sup>3</sup>),  $q_i$  is the concentration of component  $i$  in the solid phase (meq/cm<sup>3</sup>),  $t$  is the time (s),  $\varepsilon$  is the bed void fraction (-),  $K_{fi}$  is the mass transfer coefficient in the liquid film (cm/s),  $R_p$  is the radius of the particle (cm),  $U$  is the superficial fluid velocity (cm/s); (the volumetric flow rate of the fluid divided by the cross-sectional area of the bed),  $l$  is the distance along the bed (cm),  $D_{si}$  is the effective diffusivity in solid particle phase (cm<sup>2</sup>/s) and  $r$  is the radial distance in particle (cm). Equation (1) is a material balance for the ion exchange bed, while Eq. (2) is a material balance for the particle solid phase.

In general, the  $D_{si}$  diffusion coefficients are concentration dependent. There are two possibilities during simulation: (i) the diffusion coefficients are averaged over the concentration range of the experiment and thereby assumed to be constant, or (ii) they change according to the Nernst-Planck diffusion model.

$C_i^*$  is expressed in  $q_i$  by a multicomponent ion exchange equilibrium equation of the constant (or averaged) separation factor type. This if  $m$  different cations are present

$$C_i^* = \frac{C_0 \cdot \alpha_{i,1} \cdot q_i}{\sum_{k=1}^m \alpha_{k,1} \cdot q_k} \quad (3)$$

The nonlinear term  $F(q_i)$  is

$$F(q_i) = \frac{C_0 \cdot \alpha_{i,1}}{\sum_{k=1}^m \alpha_{k,1} \cdot q_k} \quad (4)$$

where  $C_0$  is the total concentration of ions in the inflow solution (meq/cm<sup>3</sup>),  $\alpha_{i,1}$  is the constant binary separation factor (normalized to component 1) and  $F(q_i)$  is a nonlinear function in Eq. (4).

The initial and boundary conditions are:

- at  $t = 0$   $q_i = 0$  for all  $r$  and  $l$  except for the saturating ion or ions for all  $t$ ,
- at  $r = 0$   $\partial q_i / \partial r = 0$  for all  $t$ ,
- at  $r = R$  for all  $t$ .

$$D_{si} \cdot \left( \frac{\partial q_i}{\partial r} \right)_{r=R_p} = K_{fi} \cdot (C_i - C_i^*) = K_{fi} \cdot [C_i - q_i \cdot F(q_i)] \quad (5)$$

Equations (1)–(5) are written for the saturation of  $m$ , where  $m$  is the number of cations in the solution. Another set of equations analogous to Eqs. (1)–(5) can be written for the regeneration (elution) step. If counter-current regeneration is employed, the term  $\partial C_i / \partial l$  in the continuity

equation must be replaced by  $\partial C_i / \partial (L - l)$ , ( $L$  is the length of the bed, cm). Assuming that the composition of the feed solution during both the saturation and regeneration steps is constant, the periodic boundary conditions for the fluid phase are:

- at  $l = 0$   $C_i = C_{i0}$  for all  $t$ , during saturation,
- at  $l = 0$   $C_i = 0$  for all  $t$ , except for the eluting ion, in the case of co-current elution,
- at  $l = L$   $C_i = 0$  for all  $t$ , except for the eluting ion, in case of counter-current elution.

The coupled, one parabolic and one hyperbolic partial differential equations can be solved using a finite difference method, as described by Mansour et al. [14] and von Rosenberg [15]. The parabolic equations can be discretized using a backward scheme, while the hyperbolic equations can be discretized with a combined scheme, first centered, then backward finite difference. The finite difference grids for the hyperbolic differential equations, using the centered finite difference scheme, are shown in Fig. 1.

$C_{l,n}$  and  $q_{l,n}$  are the fluid and solid phase concentrations at point  $l$  at old time  $n$  ( $n$  is the old time level, and  $n + 1$  denotes the new time level). According to Fig. 1 the liquid phase concentrations  $C$ , and the solid phase concentrations  $q$  were calculated by Eqs. (6) and (7).

$$C_{l-\frac{1}{2},n+\frac{1}{2}} = \frac{1}{2} \cdot (C_{l-1,n} + C_{l,n+1}) \quad (6)$$

$$q_{l,n+\frac{1}{2}} = \frac{1}{2} \cdot (q_{l,n} + q_{l,n+1}) \quad (7)$$

The concentration  $q$  is determined at points halfway between those at which  $C$  is defined. At any given time step, all the values of  $C$  and  $q$  are known at old time  $n$ .

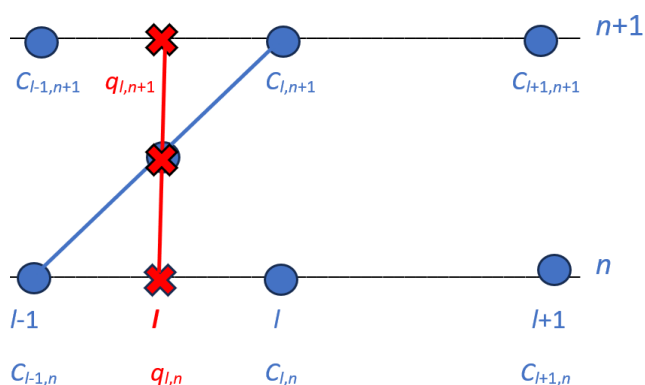


**Fig. 1** The centered finite difference grid for Eq. (1) ( $C_{l,n}$  and  $q_{l,n}$  are the fluid and solid phase concentrations at point  $l$  at old time  $n$  ( $n$  is the old time level, and  $n + 1$  denotes the new time level))

The ratio of the space increment  $\Delta l$  to the time increment  $\Delta t$  is set equal to the fluid velocity:

$$U = \frac{\Delta l}{\Delta t} \quad (8)$$

For many cases the concentration of ions in the fluid phase does not change rapidly with time, therefore, after the calculation is started, the time derivative can be omitted from Eq. (1), resulting in Eq. (9):

$$\frac{3 \cdot K_{fi}}{R_p} \cdot (C_i - C_i^*) + \frac{U}{\varepsilon} \cdot \frac{\partial C_i}{\partial l} = 0 \quad (9)$$

The backward finite difference scheme shown in Fig. 2 can discretize the Eq. (9). According to Fig. 2, the liquid phase concentrations were calculated by Eq. (10).

$$C_{l-\frac{1}{2},n+1} = \frac{1}{2} \cdot (C_{l-1,n+1} + C_{l,n+1}) \quad (10)$$

For this method, the size of the time increment is not limited by the size of the space increment. The solid phase material balances for each ion are coupled by the boundary conditions at the particle surface term through the equilibrium equation. An iterative numerical procedure was followed since the equilibrium equations are highly nonlinear. The tridiagonal system finite difference approximations of Eqs. (1)–(3) were solved by the Thomas algorithm for tridiagonal matrices. An iterative procedure is required to eliminate the nonlinearity using the finite difference equations. The denominator of the equilibrium expression is evaluated with values obtained from the previous iteration. The form

$$C_i^* = F(q_{i,it}) \cdot q_i \quad (11)$$

is linear in  $q_i$  since  $q_{i,it}$  is the  $q_i$  value obtained from the previous iteration. At the end of each iteration the value

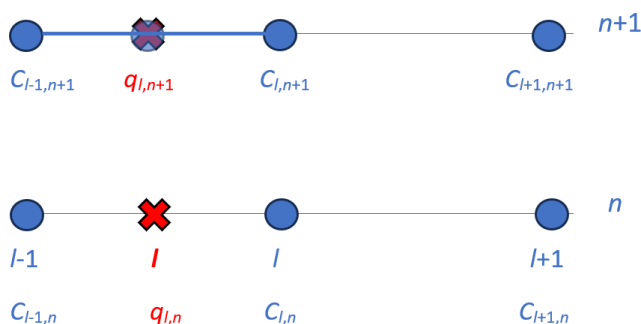


**Fig. 2** The backward finite difference grid for Eq. (9) ( $C_{l,n}$  and  $q_{l,n}$  are the fluid and solid phase concentrations at point  $l$  at old time  $n$  ( $n$  is the old time level, and  $n + 1$  denotes the new time level))

of  $q_i$  is checked to determine whether it equals  $q_i$  within a set tolerance.

The above-described multicomponent ion exchange model employs constant diffusion coefficients, which are independent of the ion concentrations within the solid particle. We added to the constant diffusion model the Nernst-Planck diffusion kinetic equation, which incorporates changing diffusion coefficients. Details of this simulation are described in [13, 16].

### 2.2 The modelling computer program

To solve this problem, we developed a computer program model and a subroutine that calculates concentration dependent diffusion coefficients using the Nernst-Planck model, as discussed in our earlier paper [13]. We consider the case of an ion exchange system exchanging  $m$  ions. With the assumptions, the following equations can be used for a given ion  $i$ :

$$J_i = -D_{si} \left( \text{grad}(q_i) + q_i z_i \frac{F}{RT} \text{grad}(\varphi) \right) \quad (12)$$

where  $J_i$  is the mass flux of ion  $i$ , (mol/(s cm<sup>2</sup>)),  $D_i$  is the individual diffusion coefficient of ion  $i$  in the exchanger (cm<sup>2</sup>/s),  $F$  is the Faraday constant (96500 C/mol),  $z_i$  is the valence of ion  $i$ ,  $R$  is the universal gas constant (8.3143 J/mol K),  $T$  is the temperature (K) and  $\varphi$  is the electric potential (V).

The initial and boundary conditions for a spherical bead are:

- at  $t = 0$   $q_i = q_{i0}$   $i = 1, n$
- at  $r = 0$   $\partial q_i / \partial r = 0$
- at  $r = R_p$   $q_i = q_{ieqs}$   $i = 1, n$ .

Where  $q_{ieqs}$  is the concentration of ion  $i$  in the exchanger at the outer surface (meq/cm<sup>3</sup>) and  $q_{i0}$  is the concentration of ion  $i$  in exchanger at  $t = 0$ , (meq/cm<sup>3</sup>).

The principle of electroneutrality requires that the total concentration of counterions, expressed in equivalents, is constant throughout the bead, hence:

$$\sum_{i=1}^m z_i q_i = Q, \quad (13)$$

where  $Q$  is the sorption capacity (exchange capacity) (meq/cm<sup>3</sup>).

The absence of an electric current inside the ion exchanger gives the condition:

$$\sum_{i=1}^n z_i J_i = 0. \quad (14)$$

From a manipulation of Eqs. (12)–(14), one obtains

$$\frac{F}{RT} \text{grad}(\varphi) = - \frac{\sum_{j=1}^m D_{sj} z_j \text{grad}(q_j)}{\sum_{j=1}^m D_{sj} z_j^2 q_j}. \quad (15)$$

Using a manipulation described in detail in [13], results instead of Eq. (2) in the following nonlinear parabolic partial differential equation:

$$\frac{\partial q_i}{\partial t} = D_{si} \cdot \frac{\partial^2 q_i}{\partial r^2} + \frac{2 \cdot D_{si}}{r} \cdot \frac{\partial q_i}{\partial r} - \frac{D_{si} z_i q_i}{(DE)} \frac{\partial A}{\partial r} \frac{\partial q_i}{\partial r} - \frac{D_{si} z_i q_i A}{(DE)} \frac{\partial^2 q_i}{\partial r^2} + \frac{D_{si} z_i q_i (NU)}{(DE)^2} \frac{\partial (DE)}{\partial r} \quad (16)$$

$$\frac{\partial q_i}{\partial r} = \frac{\partial q_{it_i}}{\partial r} \quad (17)$$

$$A = \sum_{j=1}^m D_{sj} z_j \frac{\partial q_j}{\partial q_i} = \sum_{j=1}^m D_{sj} z_j \frac{\partial q_{it_j}}{\partial q_{it_i}} \quad (18)$$

$$DE = \sum_{j=1}^m D_{sj} z_j^2 q_j = \sum_{j=1}^m D_{sj} z_j^2 q_{it_j} \quad (19)$$

where  $q_{it_i}$  is the iteration value of  $q_i$  (meq/cm<sup>3</sup>),  $NU$  is the expression in the numerator, and  $DE$  is the expression in the denominator in Eq. (16).

### 3 Numerical solution technique

The resulting partial differential equations (PDEs) can be solved using a quasi-linear finite difference equation with "four iteration coefficients". The solution of the one parabolic and one hyperbolic PDE is based on the earlier-mentioned method suggested by von Rosenberg et al. [17]. During the solution we used four iteration coefficients  $dq_1/dr$ ,  $DE(q_{i,it})$ ,  $A(q_r, it)$  and  $F(q_{i,it})$ , where  $q_{i,it}$  is the iteration value of  $q_i$ .

The values of  $DE$  and  $A$  computed at the previous iteration level can be used to evaluate the  $q_i$  concentrations at the new iteration level. Solving the diffusion Eq. (10) along with the initial and boundary conditions gives concentration profiles for each component  $i$  ( $q_i(r,t)$ ). For a spherical bead the concentration of an ion species in the resin directly correlates with the ion exchange rate. In this model, we calculated the internal concentrations at points  $1 < j < NP1$ , where  $NP1$  is the number of grid points in the particle, while the outermost point at the surface ( $j = NP1$ ) was calculated using the PDE that includes the nonlinear equilibrium equation.

#### 4 Results and discussion

A multicomponent fixed-bed ion exchange saturation model was constructed using Nernst-Planck diffusion coefficients. Based on this new model, a computer program, GELINP, written in Lahey-Fujitsu FORTRAN, was developed and multicomponent fixed-bed breakthrough curves were calculated. Then we tested the accuracy and reality of this simulation. To demonstrate the simulation results, saturation breakthrough curves for two-, three- and five-component systems were calculated. First, we calculated the breakthrough curves for a five-component ion exchange saturation using equal particle diffusion coefficients, as well as constant and Nernst-Planck diffusion coefficients. The input parameters are shown in Table 1.

The calculated breakthrough curves are shown in Fig. 3. As shown in Fig. 3, the curves overlap because there are no differences in the ionic diffusivities.

We then calculated breakthrough curves for a theoretical three-component ion exchange with constant (noNP) and Nernst-Planck (NP) diffusion coefficients. The input parameters for these calculations are shown in Table 2, and the obtained curves are in Fig. 4. In the three-component

ion exchange component ion 1 saturates the particles in the bed at the start of saturation, and ionic components 2 and 3 are in the feed.

The column contained uniform spherical ion exchange beads with a radius of  $R_p = 0.05$  cm, and the radius was divided into 100 parts with a step size of  $\Delta R_p = 0.0005$  cm. The calculation was initiated with a time increment of  $\Delta t = 0.001$  s. The calculated breakthrough curves are shown in Fig. 4.

To control the reality of our simulation, we utilized the measured sodium breakthrough in two-component and potassium breakthrough in five-component ion exchange breakthrough data, as proposed in Hokanson's PhD work [18]. The data of input parameters in Tables 3 and 4. Using the Nernst-Planck diffusion model, we compare the simulation breakthrough curves with the measured data. The results for a  $\text{Na}^+$  binary exchange breakthrough curve on a  $\text{H}^+$ -form 55.66  $\text{cm}^3$  IRN-77 SAC (Strong Acidic Cation exchanger) column, and the  $\text{K}^+$  breakthrough in a five-component ion exchange ( $\text{Na}^+$ ,  $\text{K}^+$ ,  $\text{NH}_4^+$ ,  $\text{Ca}_2^+$ ,  $\text{H}^+$ ) on a  $\text{H}^+$ -form 183.16  $\text{cm}^3$  IRN-77 SAC column are shown in Figs. 5 and 6.

**Table 1** Parameters for ion exchange saturation of five hypothetical ionic components

Parameter	Component 1	Component 2	Component 3	Component 4	Component 5
$D_s$ ( $\text{cm}^2/\text{s}$ )	$10^{-7}$	$10^{-7}$	$10^{-7}$	$10^{-7}$	$10^{-7}$
$K_j$ ( $\text{cm}/\text{s}$ )	0.01	0.01	0.01	0.01	0.01
$\alpha_{i,1}$ (-)	1.0	2.0	4.0	8.0	16.0
$C_{i0}$ ( $\text{meq}/\text{cm}^3$ )	0.0	0.005	0.005	0.005	0.005

$R_p = 0.1$  cm,  $\Delta R_p = 0.0005$  cm,  $L = 4$  cm,  $\Delta l = 0.1$  cm,  $Q = 1.00$  meq/ $\text{cm}^3$ ,  $U = 0.1$  cm/s,  $\Delta t = 0.001$  s

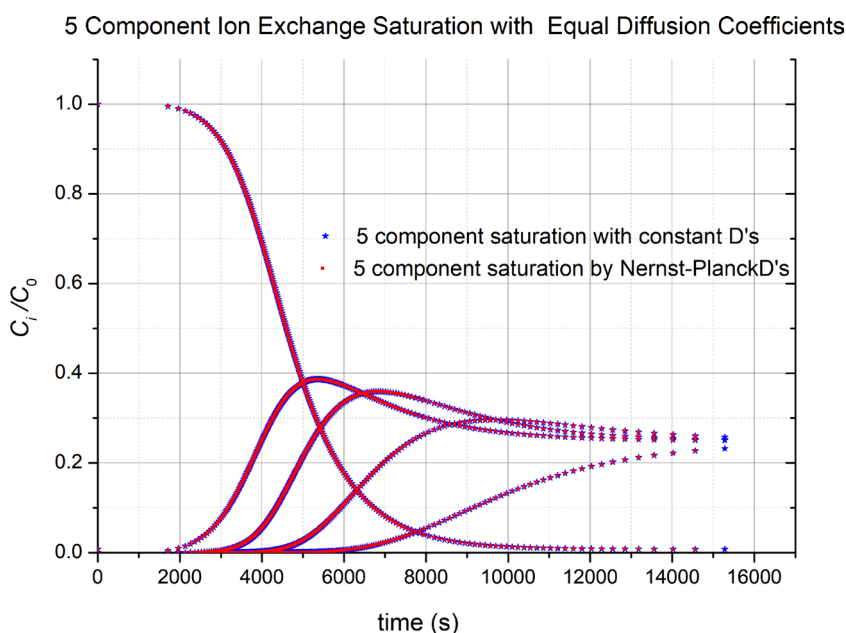


**Fig. 3** Five-component ion exchange saturation with equal diffusion coefficients

**Table 2** Parameters for saturation of three hypothetical ionic components

Parameter	Component 1	Component 2	Component 3
$D_s$ (cm <sup>2</sup> /s)	$5.0 \cdot 10^{-7}$	$4.0 \cdot 10^{-7}$	$3.0 \cdot 10^{-7}$
$K_f$ (cm/s)	0.01	0.01	0.01
$C_{i0}$ saturation (meq/cm <sup>3</sup> )	0.0	0.01	0.01
$\alpha_{i,1}$ (-)	1.0	2.0	4.0

$R_p = 0.05$  cm,  $\Delta R_p = 0.0005$  cm,  $NL = 180$ ,  $\Delta l = 0.1$  cm,  
 $Q = 1.0$  meq/cm<sup>3</sup>,  $U = 0.1$  cm/s,  $\Delta t = 0.001$  s

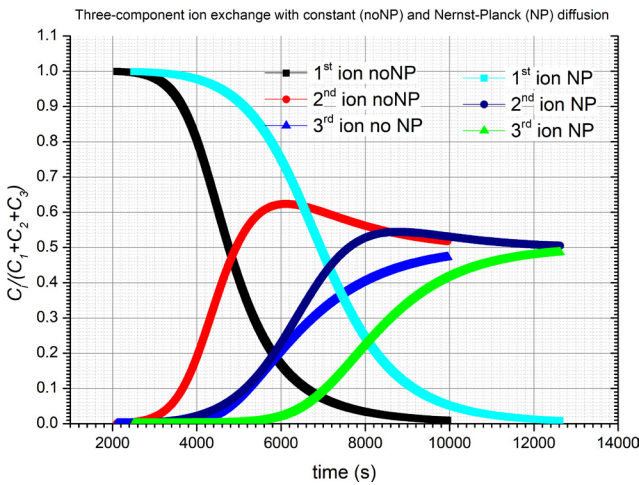


**Fig. 4** Three-component ion exchange saturation with constant and Nernst-Planck diffusion coefficients

**Table 3** Parameters for ion exchange saturation of H<sup>+</sup> exchange with Na<sup>+</sup> ion

Parameter	H <sup>+</sup>	Na <sup>+</sup>
$D_s$ (cm <sup>2</sup> /s)	$3.29 \cdot 10^{-7}$	$1.59 \cdot 10^{-7}$
$K_f$ (cm/s)	$1.48 \cdot 10^{-2}$	$9.11 \cdot 10^{-3}$
$C_{i0}$ saturation (meq/cm <sup>3</sup> )	0.0	0.0104
$\alpha_{i,1}$ (-)	1.0	1.68

$R_p = 0.02975$  cm,  $\Delta R_p = 0.0002975$  cm,  $NL = 200$ ,  $\Delta l = 0.049$  cm,  
 $Q = 2.12$  meq/cm<sup>3</sup>,  $U = 0.0405$  cm/s,  $\Delta t = 0.001$  s

**Table 4** Parameters for ion exchange saturation of H<sup>+</sup> exchanger with Na<sup>+</sup>, K<sup>+</sup>, NH<sub>4</sub><sup>+</sup>, Ca<sub>2</sub><sup>+</sup> ions

Parameter	H <sup>+</sup>	Na <sup>+</sup>	K <sup>+</sup>	NH <sub>4</sub> <sup>+</sup>	Ca <sub>2</sub> <sup>+</sup>
$D_s$ (cm <sup>2</sup> /s)	$3.29 \cdot 10^{-7}$	$1.59 \cdot 10^{-7}$	$1.97 \cdot 10^{-7}$	$1.9 \cdot 10^{-7}$	$1.32 \cdot 10^{-7}$
$K_f$ (cm/s)	$9.42 \cdot 10^{-3}$	$5.8 \cdot 10^{-3}$	$6.69 \cdot 10^{-3}$	$6.68 \cdot 10^{-3}$	$5.12 \cdot 10^{-3}$
$C_{i0}$ saturation (meq/cm <sup>3</sup> )	0.0	0.00234	0.00221	0.00268	0.00238
$\alpha_{i,1}$ (-)	1.0	1.68	2.15	1.72	59.1

$R_p = 0.02975$  cm,  $\Delta R_p = 0.0002975$  cm,  $NL = 200$ ,  $\Delta l = 0.049$  cm,  
 $Q = 2.12$  meq/cm<sup>3</sup>,  $U = 0.1256$  cm/s,  $\Delta t = 0.001$  s

The fits with the simulation for the measured sodium and potassium breakthrough curves are acceptable.

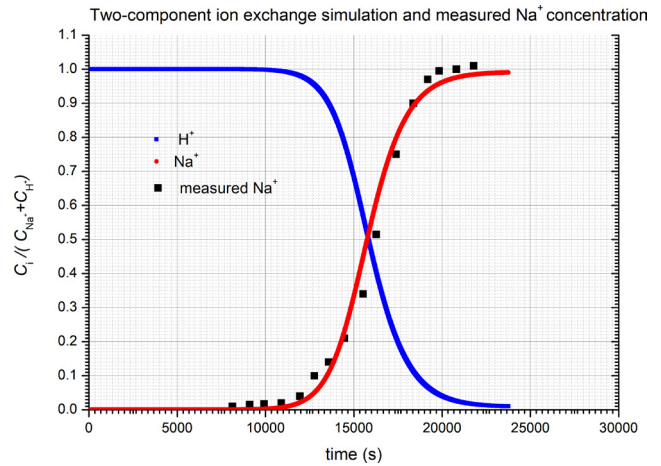


**Fig. 5** Two-component ion exchange breakthrough simulation and the measured Na<sup>+</sup> concentration

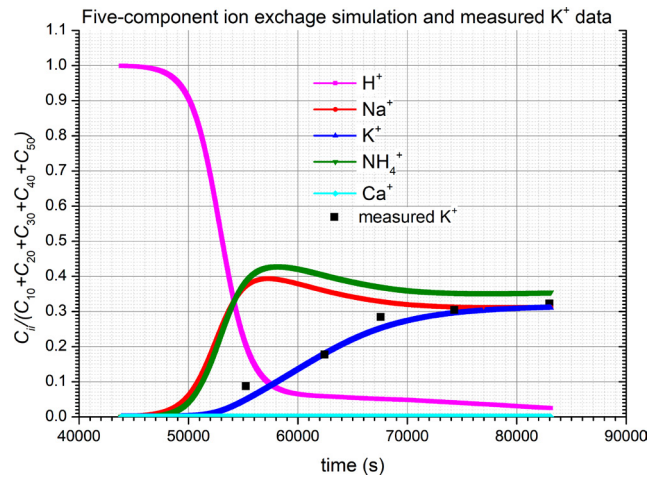


**Fig. 6** Five-component ion exchange breakthrough simulation and the measured K<sup>+</sup> concentration

### 5 Conclusion

Using our earlier developed kinetic model [13], we created a fixed-bed ion exchange model that utilized Nernst-Planck diffusion coefficients, and a computer code was constructed. The simulation program for multicomponent ion exchange in gel-type ion exchangers is applied to simulate breakthrough, using both constant and Nernst-Planck diffusion. The developed model and computational algorithm for Nernst-Planck multicomponent fixed-bed ion exchange has been tested, yielding acceptable results. The details of this new program for direct- and counter-current elution will be reported elsewhere.

## References

- [1] Evangelista, F., Di Berardino, F. C. "Modelling of Multicomponent Fixed Bed Ion Exchange Operations", In: Rodrigues, A. E. (ed.) Ion Exchange: Science and Technology, Springer, 1986, pp. 255–269. ISBN 978-94-010-8445-1  
[https://doi.org/10.1007/978-94-009-4376-6\\_9](https://doi.org/10.1007/978-94-009-4376-6_9)
- [2] Inglezakis, V. J., Zorpas, A. "Fundamentals of Ion Exchange Fixed-Bed Operations", In: Dr., I., Luqman, M. (eds.) Ion Exchange Technology I, Springer, 2012, pp. 121–161. ISBN 978-94-007-1699-5  
[https://doi.org/10.1007/978-94-007-1700-8\\_4](https://doi.org/10.1007/978-94-007-1700-8_4)
- [3] Qian, W., Wu, J., Yang, L., Lin, X., Chen, Y., Chen, X., Xiong, J., Bai, J., Ying, H. "Computational simulations of breakthrough curves in cAMP adsorption processes in ion-exchange bed under hydrodynamic flow", Chemical Engineering Journal, 197, pp. 424–434, 2012.  
<https://doi.org/10.1016/j.cej.2012.05.020>
- [4] Benedini, L. J., Furlan, F. F., Figueiredo, D., Cabrera-Crespo, J., Ribeiro, M. P. A., Campani, G., Gonçalves, V. M., Zangirolami, T. C. "A comprehensive method for modeling and simulating ion exchange chromatography of complex mixtures", Protein Expression and Purification, 205, 106228, 2023.  
<https://doi.org/10.1016/j.pep.2022.106228>
- [5] Dobre, T., Parvulescu, O. C., Calota, L., Jipa, I. "Modelling of Fixed Bed Multicomponent Ion Exchange", Revista de Chimie, 61(2), pp. 213–217, 2010.
- [6] García, E., Rodríguez, L., Ferro, V., Valverde, J. L. "Prediction of multicomponent ION exchange equilibria by using the e-NRTL model for computing the activity coefficients in solution", Fluid Phase Equilibria, 498, pp. 132–143, 2019.  
<https://doi.org/10.1016/j.fluid.2019.07.002>
- [7] Pátzay, G., Stáhl, G., Kármán, F. H., Kálmán, E. "Modelling of Scale Formation and Corrosion from Geothermal Water", Electrochimica Acta, 43(1–2), pp. 137–147, 1998.  
[https://doi.org/10.1016/S0013-4686\(97\)00242-9](https://doi.org/10.1016/S0013-4686(97)00242-9)
- [8] Pátzay, G., Zsille, O., Csurgai, J., Nényei, Á., Feil, F., Vass, G. "ILT15 - A Computer Program for Evaluation of Accelerated Leach Test Data of LLW in the Hungarian NPP Paks", Periodica Polytechnica Chemical Engineering, 63(3), pp. 527–532, 2019.  
<https://doi.org/10.3311/ppch.11714>
- [9] Pátzay, G., Nyóger, J., Zsille, O., Csurgai, J., Feil, F., Vass, G., Káta Urbán, L., Dobor, J. "ILT20 – an Upgraded Computer Program for Evaluation of Accelerated Leach Test Data of LLW in the Hungarian NPP Paks", Periodica Polytechnica Chemical Engineering, 65(4), pp. 550–558, 2021.  
<https://doi.org/10.3311/ppch.18137>
- [10] Pátzay, G., Tóth, B., Szabó, I. "Numerical Simulation of Multicomponent Ion Exchange for Porous Exchangers", Hungarian Journal of Industrial Chemistry, 17(2), pp. 153–158, 1989.
- [11] Pátzay, G., Tóth, B., Szabó, I. "Numerical Simulation of Multicomponent Ion Exchange Co-current and Counter-current elution for Porous Exchangers", Hungarian Journal of Industrial Chemistry, 20(3), pp. 179–182, 1992.
- [12] Pátzay, G., Takács, K., Jr. "Sokkomponensű szorpciós folyamatok medellezése III.: a Batchsorp program" (Modelling of the Multicomponent Sorption Processes on PC: the BATCHSORP Code), Magyar Kémikusok Lapja, 48(8), p. 354, 1993. (in Hungarian)
- [13] Pátzay, G. "A Simplified Solution Method for the Nernst-Planck Multicomponent Ion Exchange Kinetics Model", Reactive and Functional Polymers, 27(1), pp. 83–89, 1995.  
[https://doi.org/10.1016/1381-5148\(95\)00045-H](https://doi.org/10.1016/1381-5148(95)00045-H)
- [14] Mansour, A., Von Rosenberg, D. U., Sylvester, N. D. "Numerical Solution of Liquid-Phase Multicomponent Adsorption in Fixed Beds", AIChE Journal, 28(5), pp. 765–772, 1982.  
<https://doi.org/10.1002/aic.690280510>
- [15] von Rosenberg, D. U. "Methods for numerical Solution of Partial Differential Equations", Gerald L. Farrar & Associates Inc., Tulsa, OK, USA, 1978.
- [16] Pátzay, G., Csonka, E. "Research in Industrial Use of Ion Exchange and Simulation", Periodica Polytechnica Chemical Engineering, 67(4), pp. 582–591, 2023.  
<https://doi.org/10.3311/PPch.22490>
- [17] von Rosenberg, D. U., Chambers, R. P., Swan, G. A. "Numerical Solution of Surface Controlled Fixed-Bed Adsorption", Industrial & Engineering Chemistry Fundamentals, 16(1), pp. 154–157, 1977.  
<https://doi.org/10.1021/i160061a028>
- [18] Hokanson, D. R. "Development of Ion Exchange Models for Water Treatment and Application to the International Space Station Water Processor", PhD Dissertation, Michigan Technological University, 2004.  
<https://doi.org/10.37099/mtu.dc.etsds/708>